Vol. **127** (2015) *ACTA PHYSICA POLONICA A* No. 3

Electron Microscopy of Cracks in $In_xGa_{1-x}As/GaAs(001)$ Multi-Quantum Wells

Y. Atici, K. Yildiz* and U. Akgul
Firat University, Department of Physics, 23119 Elazig, Turkey

(Received March 28, 2014; in final form January 28, 2015)

We studied cracks in two different $In_xGa_{1-x}As/GaAs(001)$ multi-quantum-well structures by electron microscopy. Transmission and scanning electron microscopy analyses of the sample-1 revealed that the epilayers associated with cracks. Detailed experimental works on the cracks were carried out by conventional and high-resolution electron microscopy. It was found that the epilayers were very effective on stopping the cracks in sample-1. Many dislocations were observed around the cracks and cracks tips. SEM images showed that the cracks formed an orthogonal set array accompanying with slits and pits. However, there were not observed any cracks in the sample-2.

DOI: 10.12693/APhysPolA.127.859

PACS: 81.05.Ea, 81.07.St, 81.70.–q, 61.72.Ff

1. Introduction

The key role in defining defect formation during heteroepitaxy is the mismatch between lattice parameters and thermal expansion coefficients of two materials, which results in mechanical stresses in the structure during growth or cooling [1]. The deposition of epitaxial films grown by molecular beam epitaxy (MBE) requires annealing processes at different stages during the growth [2]. The frequently used method to reduce the dislocation density in the materials having lattice mismatch is the application of thermal annealing. However, if there is a significant difference between thermal expansion coefficients of the components, then thermal stress generating by the annealing causes the movement of dislocations through increasing the interaction between them, such as combination and annihilation, and resulting in secondary deformations in heterostructures. This could yield formation of residual stress and additional structural defects in the film [3, 4]. When thermal shock is applied to a material, cracks penetrating into the material can generate [2], but then all other crack sources can become indistinct. Thermal shock is a mechanical damage caused by mechanical stress formed by excessive temperature changes in a short time, which could not be absorbed by the structure [5].

The aim of this work was to analyse the cracks in $In_xGa_{1-x}As/GaAs(001)$ heterostructure by electron microscopy.

2. Experimental details

Two different $In_xGa_{1-x}As/GaAs(001)$ ($x \approx 0.09$) heterostructures were grown by MBE at ≈550 °C in the same conditions. The sample-1 has 10 GaAs layers with an increasing thickness at a range of 2.857–114.2857 nm. The sample-2 has 10 InGaAs layers with an increasing thickness at a range of 2.857–120 nm (Fig. 1). The sample-1 and sample-2 have ≈3.5 μm InGaAs and GaAs buffer layers, respectively. The buffer layers in the sample-1 and sample-2 were thought for relaxation in the structures. The mismatches are $f = 0.644\%$ and $f = -0.64\%$ for the sample-1 and sample-2, respectively ($a_{\mathrm{GaAs}} = 0.5653$ nm and $a_{\mathrm{InGaAs}} = 0.5689$ nm). Cross-section TEM specimens were prepared for the aim of crack and defect analyses using standard specimen preparation procedure [2]. Philips EM430 transmission electron microscope (Bristol University) and JEOL JEM2100F high-resolution TEM (Firat University) were used in this study. The surface morphologies of the specimens were investigated by a scanning electron microscope (SEM, JEOL JSM7001F).

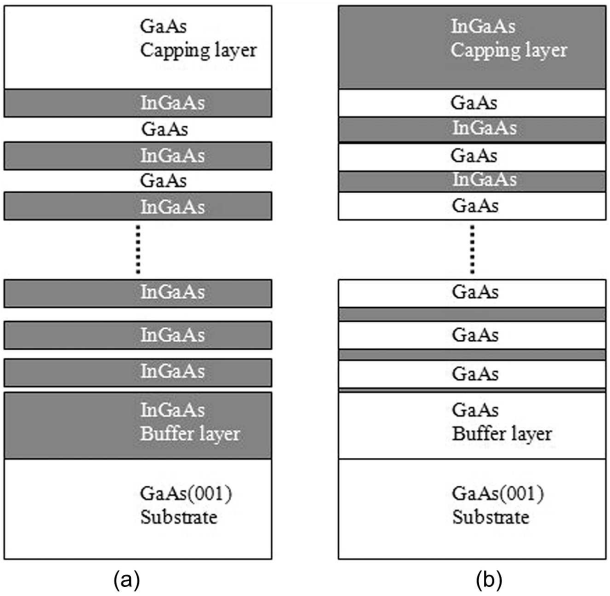

Fig. 1. Schematic representations of (a) the sample-1 and (b) the sample-2.

---

*corresponding author; e-mail: kyildiz@firat.edu.tr

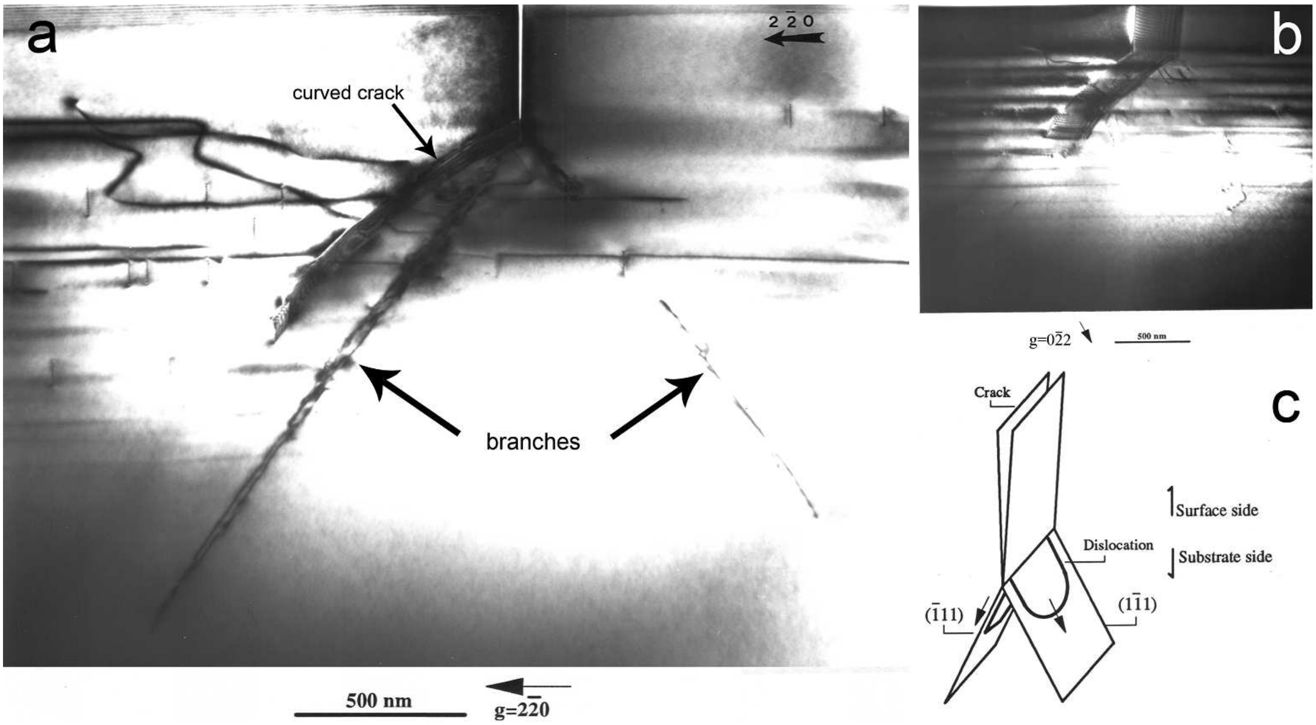

Fig. 2. (a) A bright-field image taken from a cross-section specimen of the sample-1 in $\boldsymbol{g} = 2\bar{2}0$ showing a crack associated with dislocations in the epilayers. (b) A view of the same area in Fig. 2a after tilting the specimen away from [110] (about 40°) towards [100]. The diffraction vector is $\boldsymbol{g} = 0\bar{2}2$. (c) A schematic diagram showing the dislocation generation from the crack tip.

3. Results and discussion

Figure 2a shows a cross-section TEM image of a crack penetrating from the surface of the GaAs capping layer into the InGaAs and GaAs epilayer with branches in the epilayers of the sample-1 taken in $\boldsymbol{g} = 2\bar{2}0$. The cracks run through the capping layer into the top InGaAs epilayer in the growth direction (001). In this direction, the crack is about 400 nm in length. In the first InGaAs layer, the crack changes its direction ($\approx 58°$) running into the other epilayers with a curve shaped of ≈ 900 nm in length ending in an InGaAs epilayer. The cracks in GaAs structures are on $\{110\}$ planes [6–8].

Cracks in heterostructures are associated with dislocations. These dislocations can be observed around the cracks and cracks tips in the structures and the nucleation and propagation of dislocations can be attributed to the cracks [8–11]. These dislocations which have been generated from the point in which the crack changes its direction can be seen in Fig. 2a. These dislocations are on the two different slip planes running down through the epilayers towards the substrate. The Burgers vectors of these dislocations were found to be $\boldsymbol{b} = 1/2[\bar{1}01], 1/2[011], 1/2[101] and 1/2[0\bar{1}1]$ and in addition the slip planes of these dislocations are either of $(1\bar{1}1)$ and $(\bar{1}11)$.

Tilt experiments were performed in the microscope in order to analyse the dislocations and cracks. The specimen was tilted away from the [100] zone axis ($\approx 40°$) to a two-beam condition was for $\boldsymbol{g} = 0\bar{2}2$. The bright-field image in Fig. 2b shows the crack and dislocations in two-beam condition. The micrograph demonstrates the points at which the crack changes its direction ending in the epilayers as well as dislocation generation around the crack. The micrograph also clearly shows that no cracks associated with dislocations formed in two bunches on $(1\bar{1}1)$ and $(\bar{1}11)$ planes running towards the substrate. Figure 2c illustrates dislocation nucleation schematically. Furthermore, the overlapping crack faces formed Moire fringes as seen in Fig. 2b. These dislocations lead to strain relaxation in the epilayers. The cracks in Fig. 2a were deflected by the first InGaAs layer. The strain left in the layer could be found to be 0.5601%, taking a strain relaxation of 0.062%. Dislocation separation in the layer was also found to be 320 nm [2]. Atici [12, 13] also reported dislocations spacings of 390–666 nm and 342–1000 nm for the epilayer interfaces of the sample-1 and sample-2, respectively. These results imply less strain relaxation by the misfit dislocations in the sample-1 compared to the sample-2. As seen in the results, the strain relaxation in the sample-1 also occurred significantly by the crack formation. Hearne et al. [14] demonstrated that the crack initiation caused the formation of misfit dislocations at the film/substrate interface and thus the strain relaxation could be easily explained.

We observed the cracks changing their planes and propagate in the different (110) and (113) planes emitting dislocations into the structure (Fig. 3). The micrograph is a dark-field image taken in $\boldsymbol{g} = 2\bar{2}0$. As shown in the micrograph, each of the cracks has two brunches associated with dislocations in the epilayers as well as in the capping layer. The two cracks in Fig. 3 have equal length of about 1030 nm in the layers parallel to [001]. They both spilt into two branches exactly in the same epilayer which is InGaAs, 120 nm in thickness. The angle between the two branches was measured to be almost 125° for both cracks. Furthermore, the angle between a branch normal and the growth direction [001] of 25° indicates that each one of the branches of the cracks are on two different (113) planes. The branches on these planes have length of 685, 400, 400 and 257 nm, respectively. A similar crack structure in InGaP/GaAs was also observed by Wang et al. [15]. Their observation indicated that the crack could move on different planes. Salviati et al. [16] reported the strain relaxation mechanisms in $In_xGa_{1-x}As$/InP heterostructures under tensile and compressive strain. They demonstrated that the cracks, which have exhibited a different density along [110] and [$1\bar{1}0$] depending on the residual strain, occurred after growth, and however, that the cracks did not have an important contribution to the strain relaxation inside the structures. Yang et al. [17] observed an asymmetric crack array formation, caused by high thermal mismatches between in GaAs films grown on Si and SiGe virtual substrates. Murray et al. [18] reported a simple model describing the formation of cracks and their structural properties in tensile strained epilayers. This model has been found in accordance with experimental observations on III–V compounds.

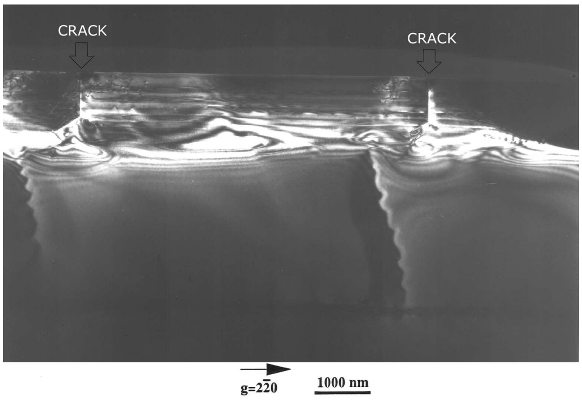

Fig. 3. A dark-field image demonstrating two cracks with branches in $\boldsymbol{g} = 2\bar{2}0$ in the sample-1.

Figure 4a displays a HRTEM image of a crack taken from the [011] zone axis. No defects were observed around this crack, but we could see some stacking faults at the tip of crack. A HRTEM image of the tip of the same crack is shown in Fig. 4b. The areas having crystallographic irregularities were marked by white circles. These defects at the crack tip can enable the reducing the overall energy with the increment of the stress [19].

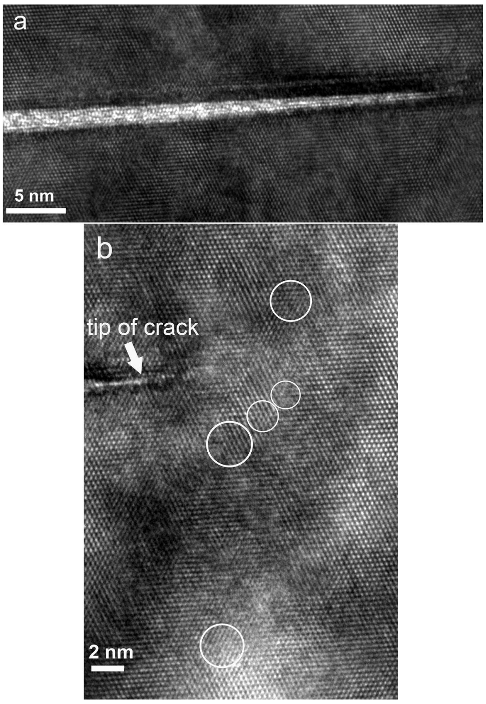

Fig. 4. HRTEM images taken from (a) around and (b) tip of a crack in the GaAs capping layer of the sample-1.

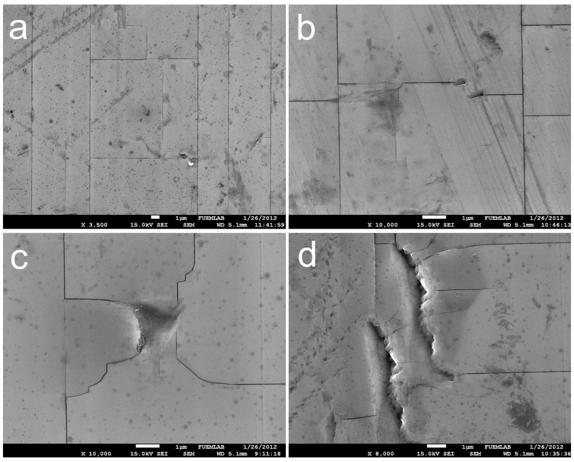

Fig. 5. SEM images taken from different regions on the surface of the sample-1 showing many cracks, slits and pits. The sample-1 exhibits an orthogonal crack array.

Figure 5 depicts SEM images of cracks on the surface of sample-1. The cracks forming an orthogonal set are shown in Fig. 5a. Their propagations could be influenced by the structural deformities, such as pits and slits (Fig. 5b). Many surface pits and slits were detected in different SEM specimens, as well. Two of them were imaged in Fig. 5c and d. Due to additional stresses generated by these micro pits and slits, new shorter micro surface cracks were nucleated around them and also some cracks changed their propagation directions.

SEM and TEM analyses of the sample-2 indicated that there were no any cracks and structural deformities in the sample-2 (SEM image not shown). Figure 6 depicts a cross-section TEM micrograph of the sample-2. The SEM and TEM results are in a good agreement.

Consequently, the sample-2 has no cracks. Even though the sample-1 and the sample-2 were grown in the same condition, we suggested that the reason of cracks in the sample-1 could be due to the different sequences of GaAs and InGaAs layers.

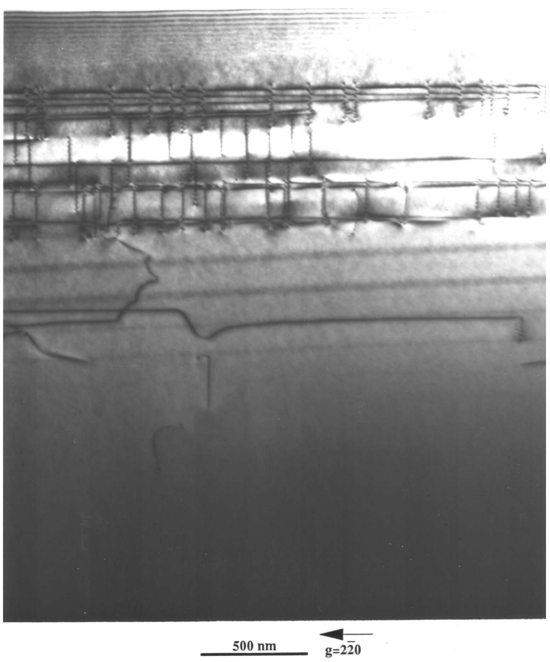

Fig. 6. A bright-field micrograph of a cross-section specimen of the sample-2.

The presence of cracks in the sample-1 could be also attributed to a thermal shock and strain in the epilayers as well as lattice mismatch between GaAs and InGaAs. As a result of thermal shock by thermal annealing, thermal stress and strain are randomly generated on the surface of material. Thus, the surface of material stores the strain energy [20]. Thermal strain depends on the thermal expansion coefficients of the film and substrate [21]. Especially, crack arrays in the thin films are the result of high thermal mismatch [17]. Consequently, the strain energy in the structure can be relaxed via crack initiation [20].

4. Conclusions

It was seen that the crack formation depended strongly on the sequences of InGaAs and GaAs epilayers. The cracks in sample-1 changed their planes and propagate in the different {110} and {113} planes having one or more branches associated with dislocations, gliding on {111} slip planes in the structure. The SEM images of sample-1 revealed the cracks in the form of an orthogonal set accompanying with slits and pits. The strain relaxation significantly occurred by the crack formation in the sample-1. However, no cracks were observed in the sample-2.

Acknowledgements

We would like to thank Professor David Cherns for many useful discussions (H.H. Wills Physics Laboratory, Bristol University UK).

References

[1] I.V. Kurilo, S.K. Guba, *Inorg. Mater.* **47**, 819 (2011).

[2] Y. Atici, Ph.D. Thesis, University of Bristol, UK 1993.

[3] A.N. Buzynin, Y.N. Buzynin, A.V. Belyaev, A.E. Luk'yanov, E.I. Rau, *Thin Solid Films* **515**, 4445 (2007).

[4] T. Sasaki, K. Arafune, W. Metzger, M.J. Romero, K. Jones, M. Al-Jassim, Y. Ohshita, M. Yamaguchi, *Sol. En. Mater. Sol. Cells* **93**, 936 (2009).

[5] J. Maxwell, in: *Proc. 38th Electronics Components Conf. 1988*, IEEE, Los Angeles 1988, p. 376.

[6] J.W. Matthews, A.E. Blakeslee, *J. Cryst. Growth* **32**, 265 (1976).

[7] K. Yasutake, Y. Konishi, K. Adachi, K. Yoshi, M. Umeno, H. Kawabe, *Jpn. J. Appl. Phys.* **27**, 2238 (1988).

[8] S. Fujita, K. Maeda, S. Hyodo, *Philos. Mag. A* **65**, 131 (1992).

[9] G. Michot, A. George, *Inst. Phys. Conf. Series* **104**, 385 (1989).

[10] D.R. Clarke, R.F. Cook, *Inst. Phys. Conf. Series* **104**, 397 (1989).

[11] D.R. Clarke, Y.H. Chiao, *Ultramicroscopy* **29**, 203 (1989).

[12] Y. Atici, *Balkan Phys. Lett.* **3**, 91 (1995).

[13] Y. Atici, *J. Cryst. Growth* **156**, 147 (1995).

[14] S.J. Hearne, J. Han, S.R. Lee, J.A. Floro, D.M. Follstaedt, E. Chason, I.S.T. Tsong, *Appl. Phys. Lett.* **76**, 1534 (2000).

[15] J. Wang, J.W. Steeds, M. Hopkinson, *Semicond. Sci. Technol.* **8**, 502 (1993).

[16] G. Salviati, C. Ferrari, L. Lazzarini, L. Nasi, A.V. Drigo, M. Berti, D. De Salvador, M. Natali, M. Mazzer, *Appl. Surf. Sci.* **188**, 36 (2002).

[17] V.K. Yang, M. Groenert, C.W. Leitz, A.J. Pitera, M.T. Currie, E.A. Fitzgerald, *J. Appl. Phys.* **93**, 3859 (2003).

[18] R.T. Murray, C.J. Kiely, M. Hopkinson, *Semicond. Sci. Technol.* **15**, 325 (2000).

[19] G. Schoeck, *J. Mech. Phys. Solids* **44**, 413 (1996).

[20] S. Shimamura, Y. Sotoike, *J. Mater. Res.* **7**, 1286 (1992).

[21] Z. Suo, *Encyclop. Mater. Sci. Technol.* **4**, 3290 (2001).